

Supplementary materials for the main submission entitled -
 Detecting distributional differences between temporal granularities
 for exploratory time series analysis

Contents

1	Recalling notations	1
2	Raw weighted pairwise distance	2
2.1	Tuning parameter	2
2.2	Underlying distributions	2
2.3	Number of comparisons	3
3	Adjusted weighted pairwise distances	3
3.1	Permutation approach	3
3.2	Modeling approach	4
3.3	Combination approach	4
4	Ranking and selecting harmonies	4

1 Recalling notations

Let $v = \{v_t : t = 0, 1, 2, \dots, T - 1\}$ be a continuous measured variable observed across T time points. The number of cyclic granularities considered in the display (at once) is m . Consider cyclic granularities A and B , such that $A = \{a_j : j = 1, 2, \dots, J\}$ and $B = \{b_k : k = 1, 2, \dots, K\}$. For $m = 1$, only one of A or B is plotted at once and a *panel* refers to a display of distributions of v across J or K levels on the x-axis. For $m = 2$, the distribution display of v with A placed across x-axis and B across facets is referred to as a (J, K) panel (J x-axis levels and K facet levels). The pairwise distances between pairs $(a_j b_k, a'_j b'_k)$ could be within-facets or between-facets as seen in Figure 4 of the main paper. The tuning parameter, used to put relative weight-age to the pairwise distances within and between facets is denoted by λ . Let the four elementary designs be D_{null} where there is no pairwise difference in distribution of v across A or B , D_{var_f} denotes the set of designs where there is difference in distribution of v for B and not for A . Similarly, D_{var_x} denotes the set of designs where difference is observed only across A . Finally, $D_{var_{all}}$ denotes those designs for which difference is observed across both A and B . The following method is deployed for generating different distributions across different combinations for non-null designs - suppose the distribution of the combination of first levels of x and facet category is $N(\mu, \sigma)$ and μ_{jk} denotes the mean of the combination $(a_j b_k)$, then $\mu_{j.} = \mu + j\omega$ (for design D_{var_x}) and $\mu_{.k} = \mu + k\omega$ (for design D_{var_f}), where ω denotes the increment in mean. Table 1 shows an example of how designs are defined for a $(2, 3)$ panel using $\omega = 3$. nx and $nfacet$ denotes the number of categories placed on x-axis and facets respectively. wpd_{raw} and wpd denote the raw and normalized weighted pairwise distances.

Table 1: Simulation setup for a panel with 3 facet levels and 2 x-axis levels for different designs starting from an initial distribution $N(0, 1)$ for the combination (a_1, b_1) and $\omega = 3$.

x levels	facet levels	D_{null}	D_{var_f}	D_{var_x}	$D_{var_{all}}$
a_1	b_1	$N(0, 1)$	$N(0, 1)$	$N(0, 1)$	$N(0, 1)$
a_2	b_1	$N(0, 1)$	$N(0, 1)$	$N(3, 1)$	$N(3, 1)$
a_1	b_2	$N(0, 1)$	$N(3, 1)$	$N(0, 1)$	$N(6, 1)$
a_2	b_2	$N(0, 1)$	$N(3, 1)$	$N(3, 1)$	$N(9, 1)$
a_1	b_3	$N(0, 1)$	$N(6, 1)$	$N(0, 1)$	$N(12, 1)$
a_2	b_3	$N(0, 1)$	$N(6, 1)$	$N(3, 1)$	$N(15, 1)$

2 Raw weighted pairwise distance

2.1 Tuning parameter

For $m = 1$, pairwise distances could be defined only between different categories of the cyclic granularity considered. So no tuning parameter is applicable for this case. For $m = 2$, λ might impact wpd_{raw} differently depending on the value of ω and different values of nx , $nfacet$ and designs. The following simulation study sees the impact of λ for different ω , nx , $nfacet$ and designs.

Simulation design

Observations are generated from $N(0,1)$ distribution for each combination of nx and $nfacet$ from the following sets: $nx = nfacet = \{2, 3, 5, 7\}$ and wpd_{raw} is computed for $\lambda = 0.1, 0.2, \dots, 0.9$ under two designs D_{var_x} and D_{var_f} for $\omega = \{1, 8\}$ to observe how the value of wpd_{raw} changes for different designs. Moreover, to observe for which value of λ the two designs intersect, we generate observations from $N(0,1)$ distribution for each combination of nx and $nfacet$ from the following sets: $nx = nfacet = \{2, 3, 5, 7, 14, 20\}$ and $\omega = \{1, 2, \dots, 10\}$ under the same two designs.

Results

Figure 1 shows how the value of wpd changes for $\lambda = 0.1, 0.2, \dots, 0.9$ for the two different designs D_{var_x} and D_{var_f} for two values of increment in mean $\omega = 1, 8$. For a lower value of ω , the two designs intersect at $\lambda > 0.7$ and for a higher ω , the two designs intersect at $\lambda = 0.5$. The value of wpd increases with λ for D_{var_x} and decreases with increasing λ for D_{var_f} . Figure 2 shows the value of λ for which the two designs intersect for different values of ω . It can be observed that as the value of ω ($\omega > 4$) increase, the value of λ at which the two designs intersect converge is $\lambda = 0.5$ and for ω ($\omega \leq 4$), designs interact between $\lambda = [0.6, 0.75]$. Hence, $\lambda = 0.67$ is used for the rest of the paper, which is an average of the range of values λ can take in order to have equal or more weightage for the within-facet distances.

2.2 Underlying distributions

The following simulation study sees the impact of different underlying distributions on wpd_{raw} for different nx and $nfacet$ before and after performing Normal Quantile Transformation.

Simulation design

Observations are generated from $N(0,1)$, $N(5, 1)$, $N(0, 5)$, $\text{Gamma}(0.5, 1)$ and $\text{Gamma}(2, 1)$ distributions for each combination of nx and $nfacet$ from the following sets: $nx = nfacet = \{2, 3, 5, 7, 14, 20, 31, 50\}$ and wpd_{raw} is computed with $\lambda = 0.67$ with (scenario 1) and without (scenario 2) NQT.

Results

Figure 3 shows ridge plots of wpd_{raw} for a $\text{Gamma}(0.5, 1)$, $\text{Gamma}(2, 1)$ before NQT. It is observed that for the underlying distribution $\text{Gamma}(2, 1)$, location and scale of the distribution of wpd changes from top-left panel to bottom-right panel. Figure 4 shows the the distributions of wpd under same underlying distributions

after performing NQT. It is observed that within each panel, the distributions of the wpd looks same, however, the distributions change from extreme top-left panel to bottom-right panels. Similar observations could be made in Figure 5 for different underlying normal distributions $N(0,1)$, $N(5,1)$ and $N(0,5)$. This implies, NQT has atleast been able to make the location and scale of the distribution of wpd_{raw} same for different underlying distributions.

2.3 Number of comparisons

2.3.1 Case: $m = 1$

Simulation design

Observations are generated from a $N(0,1)$ distribution for each $nx = \{2, 3, 5, 7, 9, 14, 17, 20, 24, 31, 42, 50\}$ to cover a wide range of levels from very low to moderately high. $ntimes = 500$ observations are drawn for each combination of the categories, that is, for a panel with $nx = 3$, 500 observations are simulated for each of the categories. This design corresponds to D_{null} as each combination of categories in a panel are drawn from the same distribution. Furthermore, the data is simulated for each of the categories $nsim = 200$ times, so that the distribution of wpd under D_{null} could be observed. The values of wpd is obtained for each of the panels. $wpd_{l,s}$ denotes the value of wpd obtained for the l^{th} panel and s^{th} simulation.

Results

Figure 6 shows ridge plots of wpd_{raw} for an underlying $N(0,1)$ distribution. For each panel, it could be seen that the location shifts to the right for increasing x levels. Across each panel, the scale of the distribution seems to change for low/moderately from lower values to higher values of nx and left tails are longer for lower facet levels.

2.3.2 Case: $m = 2$

Simulation design

Similarly, observations are generated from a $N(0,1)$ distribution for each combination of nx and $nfacet$ from the following sets: $nx = nfacet = \{2, 3, 5, 7, 14, 20, 31, 50\}$. That is, data is being generated for each of the panels $(2, 2), (2, 3), (2, 5) \dots, (50, 31), (50, 50)$. For each of the 64 panels, $ntimes = 500$ observations are drawn for each combination of the categories. That is, if we consider a $(2, 2)$ panel, 500 observations are generated for each of the possible subsets, namely, $\{(1, 1), (1, 2), (2, 1), (2, 2)\}$.

Results

Figures 8, 9 and 10 shows the ridge plot of wpd_{raw} with nx as facets, $nfacet$ as facets and the density plot of wpd_{raw} with nx on the x-axis and $nfacet$ on the facets. The right-ward shift in location can be clearly observed from all figures.

3 Adjusted weighted pairwise distances

Simulation design

This sections shows the result from the different approaches of adjusting for the number of comparisons. Simulation design is the same as for raw weighted pairwise distances for $m = 1$ and $m = 2$. In place of wpd_{raw} , wpd_{perm} , wpd_{glm} and wpd is computed for all panels.

3.1 Permutation approach

Figure 11 and 12 show the normalized wpd for $m = 1$ and $m = 2$ respectively. The location and scale are brought to similar values for increasing values of nx or $nfacet$. Due to heavy computational load, wpd_{perm} for few panels with very high value of nx or $nfacet$ are not computed.

Table 2: Results of generalised linear model to capture the relationship between wpd_{raw} and number of comparisons for $m = 1$.

distribution	term	estimate	std.error	statistic	p.value
N(0, 1)	(Intercept)	26.086352	0.5397440	48.330973	0.0e+00
N(0, 1)	log('nx * nfacet')	-1.874597	0.1894537	-9.894751	1.8e-06

Table 3: Results of generalised linear model to capture the relationship between wpd_{raw} and number of comparisons for different underlying distribution.

distribution	term	estimate	std.error	statistic	p.value
Gamma(0.5, 1)	(Intercept)	23.67	0.242	97.95	0
Gamma(0.5, 1)	log('nx * nfacet')	-1.01	0.049	-20.88	0
Gamma(2, 1)	(Intercept)	23.69	0.240	98.77	0
Gamma(2, 1)	log('nx * nfacet')	-1.02	0.048	-21.24	0
N(0, 1)	(Intercept)	23.40	0.225	104.14	0
N(0, 1)	log('nx * nfacet')	-0.96	0.044	-21.75	0
N(0, 5)	(Intercept)	23.56	0.221	106.71	0
N(0, 5)	log('nx * nfacet')	-1.00	0.044	-22.45	0
N(5, 1)	(Intercept)	23.56	0.221	106.71	0
N(5, 1)	log('nx * nfacet')	-1.00	0.044	-22.45	0
N(5, 5)	(Intercept)	23.56	0.221	106.71	0
N(5, 5)	log('nx * nfacet')	-1.00	0.044	-22.45	0

3.2 Modeling approach

For $m = 1$, Figure 13 shows the scatterplot of wpd_{raw} against different values of nx and also the display of residuals from the model and Figure 14 shows the distribution of wpd_{glm} for different nx . For $m = 2$, Figure 15 shows the scatterplot of wpd_{raw} against different values of nx and also the display of residuals from the model. Figure 16 shows the distribution of wpd_{glm} for different nx .

3.3 Combination approach

3.3.1 Results

“The distribution of wpd_{perm} and wpd_{glm_scaled} are overlaid to compare the location and scale across different nx and $nfacet$. wpd_{norm} takes the value of wpd_{perm} for lower levels (≤ 5), and wpd_{glm_scaled} for higher levels to alleviate the problem of computational time in permutation approaches. This is possible as the distribution of the adjusted measure looks similar for both approaches for higher levels.”

4 Ranking and selecting harmonies

Simulation design

Observations are generated from a $N(0,1)$ distribution for each combination of nx and $nfacet$ from the following sets: $nx = \{3, 7, 14\}$ and $nfacet = \{2, 9, 10\}$. This would result in 9 panels, viz, $(3, 2), (3, 9), (3, 10), \dots, (14, 9), (14, 10)$. Few experiments were conducted. In the first scenario, data for all panels are simulated using the null design D_{null} . In other scenarios, data simulated from the panel $(14, 2)$ and $(3, 10)$ are under $D_{varyall}$. Moreover, $\omega = \{0.5, 2, 5\}$ are considered to examine if the proposed test is able to capture subtle differences and non-subtle differences when we shift from the null design. In the last scenario, we consider the panel $(3, 2), (7, 9), (14, 10)$ to be under D_{null} , the panels $(7, 2), (14, 9)$ to be under D_{varf} , $(14, 2), (3, 10)$ under D_{varx} and the rest under $D_{varnull}$. This is done to check if the consequent ranking procedure leads to designs like $D_{varyall}$ to be chosen first followed by $D_{varyall}$. We generate only one

data set each for which these scenarios were simulated and consider this as the original data set. We generate 1000 repetitions of this experiment with different seeds.

Results

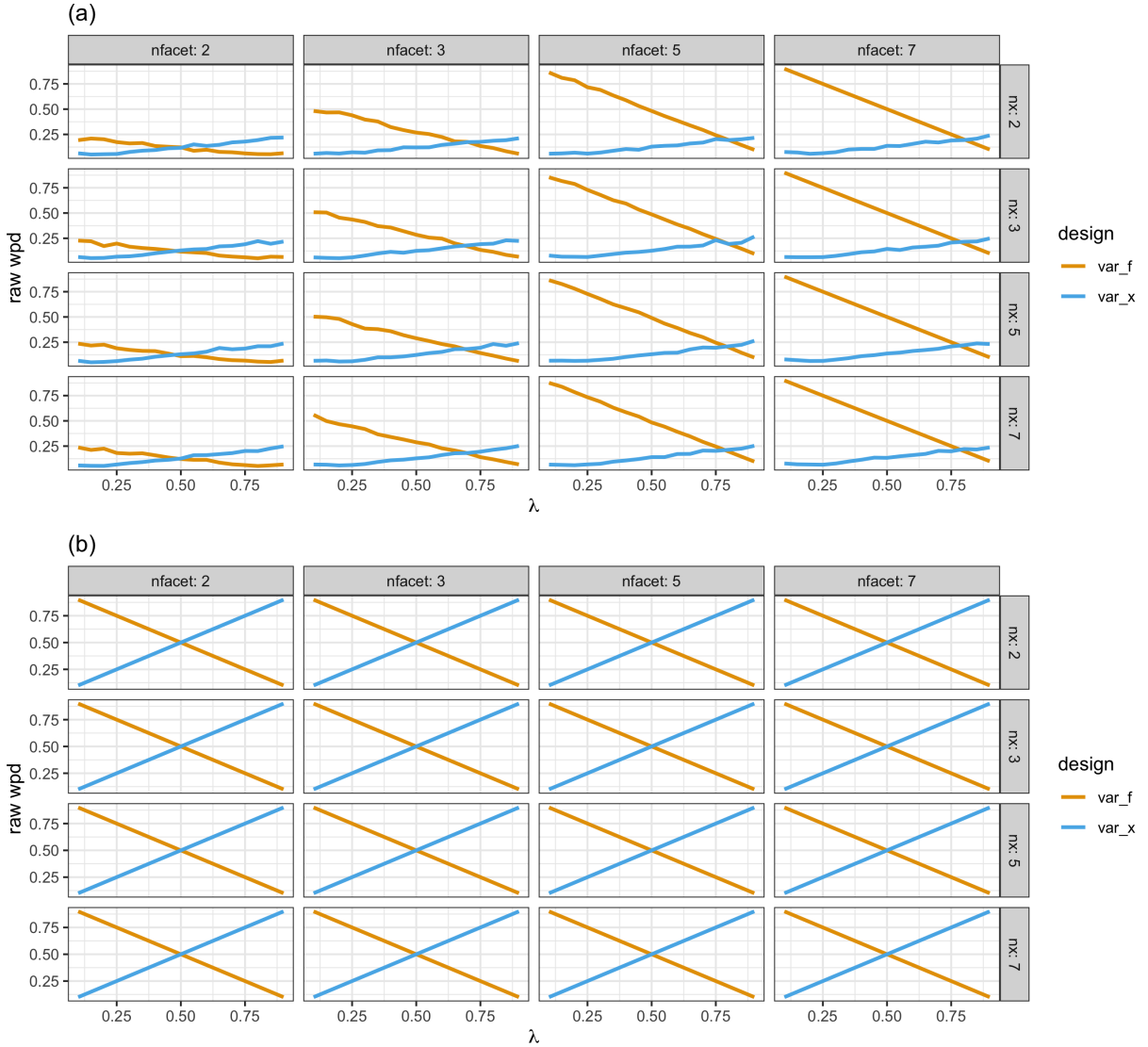


Figure 1: wpd_{raw} from two designs are plotted for different values of λ nx and $nfacet$. For $\omega = 1$, the designs intersect for $0.6 < \lambda \leq 0.75$, whereas for higher omega, design intersects at $\lambda = 0.5$.

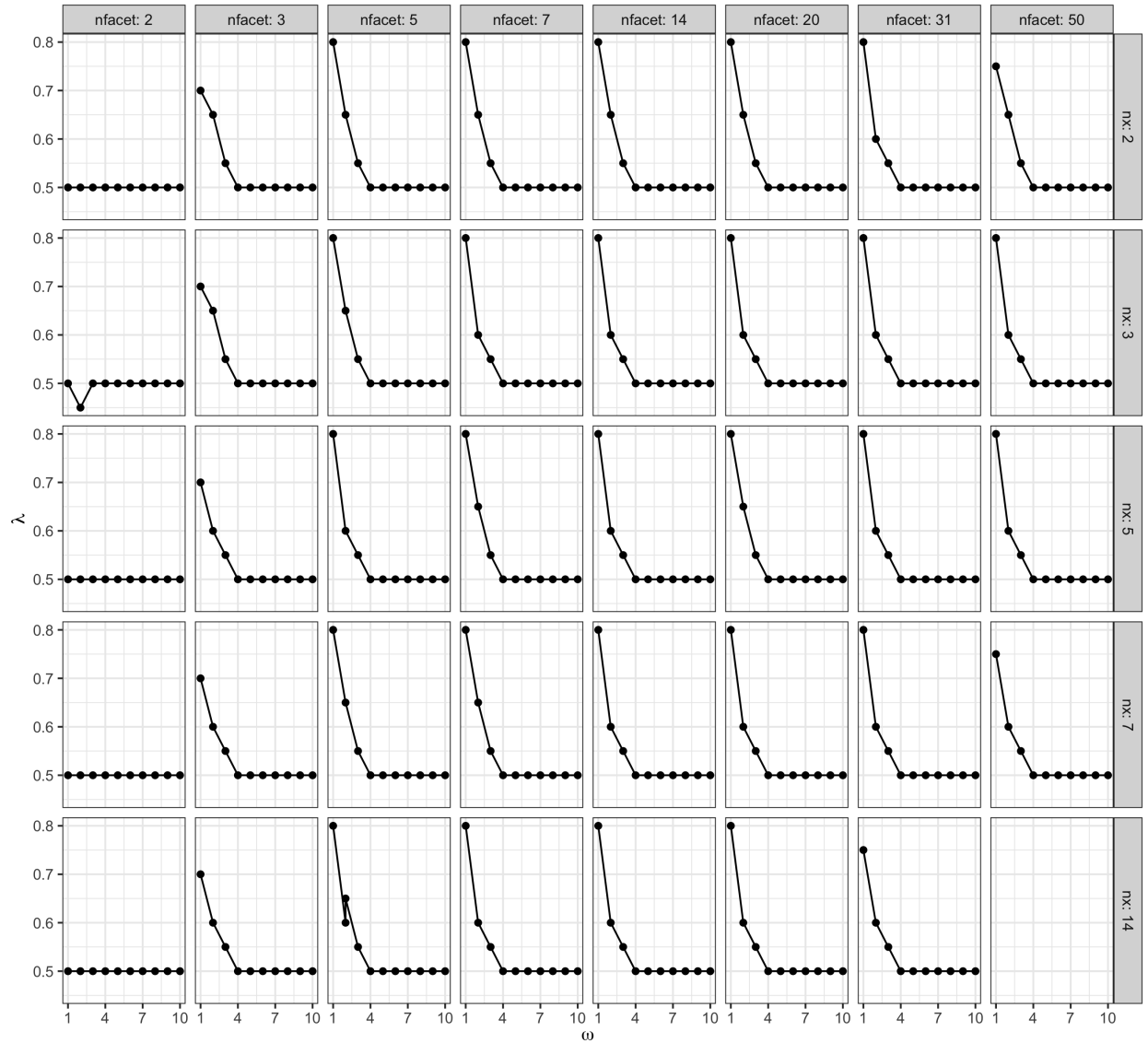


Figure 2: The point of intersection of wpd_{raw} values under the designs D_{var_f} and D_{var_x} are plotted across different ω and λ . For most panels it is observed that a common value of λ for which the designs interact is 0.5 for $\omega \geq 4$, which implies any value greater than 0.5 could be chosen to up-weight the within-facet distances and down-weigh the between-facet distances. The value of λ is higher for $\omega < 4$ could be anywhere between 0.6 and 0.75.

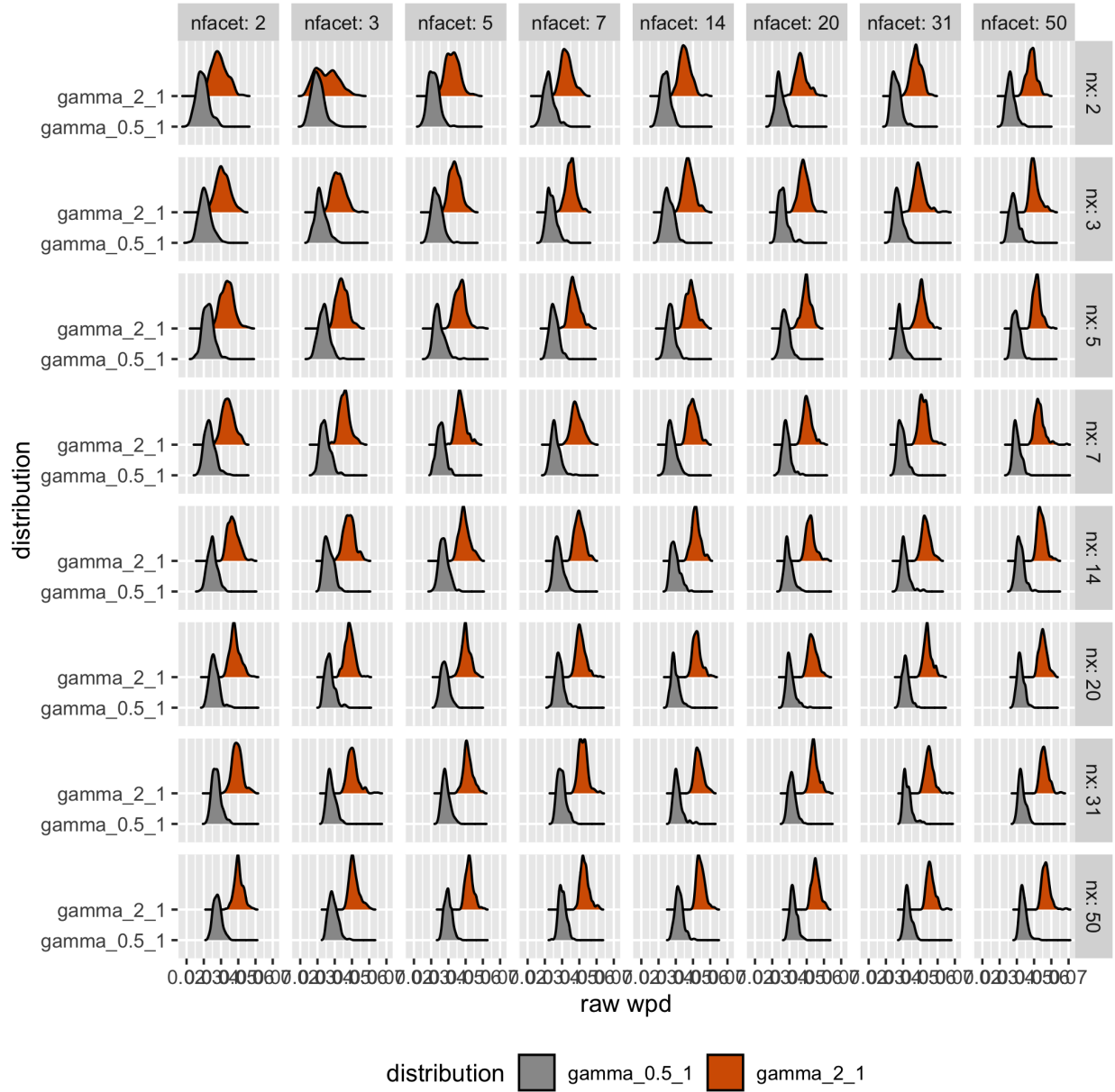


Figure 3: Ridge plots of raw wpd is shown for Gamma(0.5,1), Gamma(2,1) distribution without NQT. The densities change across different facet and x levels and also looks different for the two distributions, which implies wpd value is affected by the change in the shape parameter of the gamma distribution.

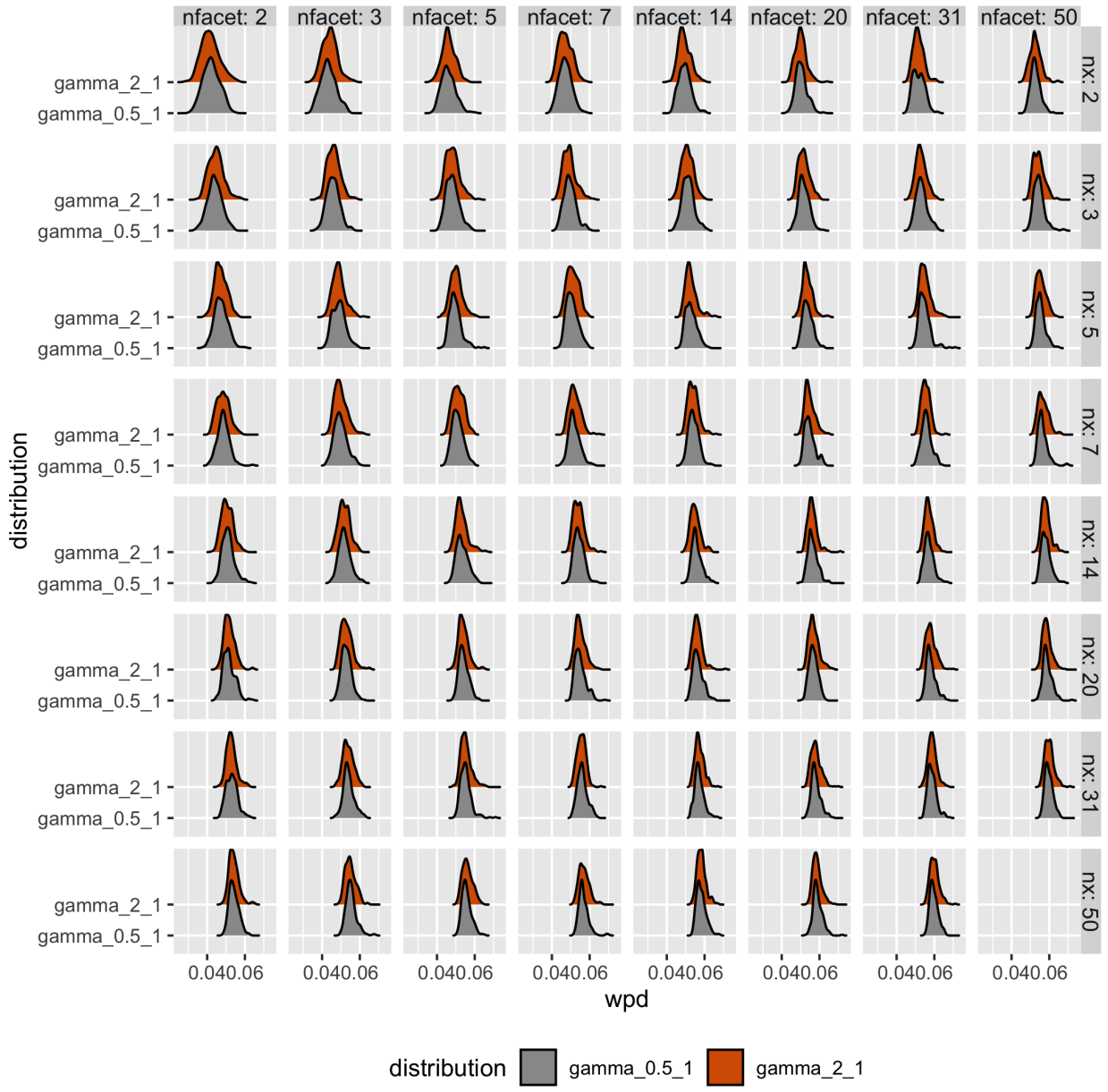


Figure 4: Ridge plots of raw wpd is shown for $\text{Gamma}(0.5, 1)$, $\text{Gamma}(2, 1)$ distribution. The densities change across different facet and x levels but look same for the two distributions, which implies wpd value is unaffected by the change in the shape parameter of the gamma distribution

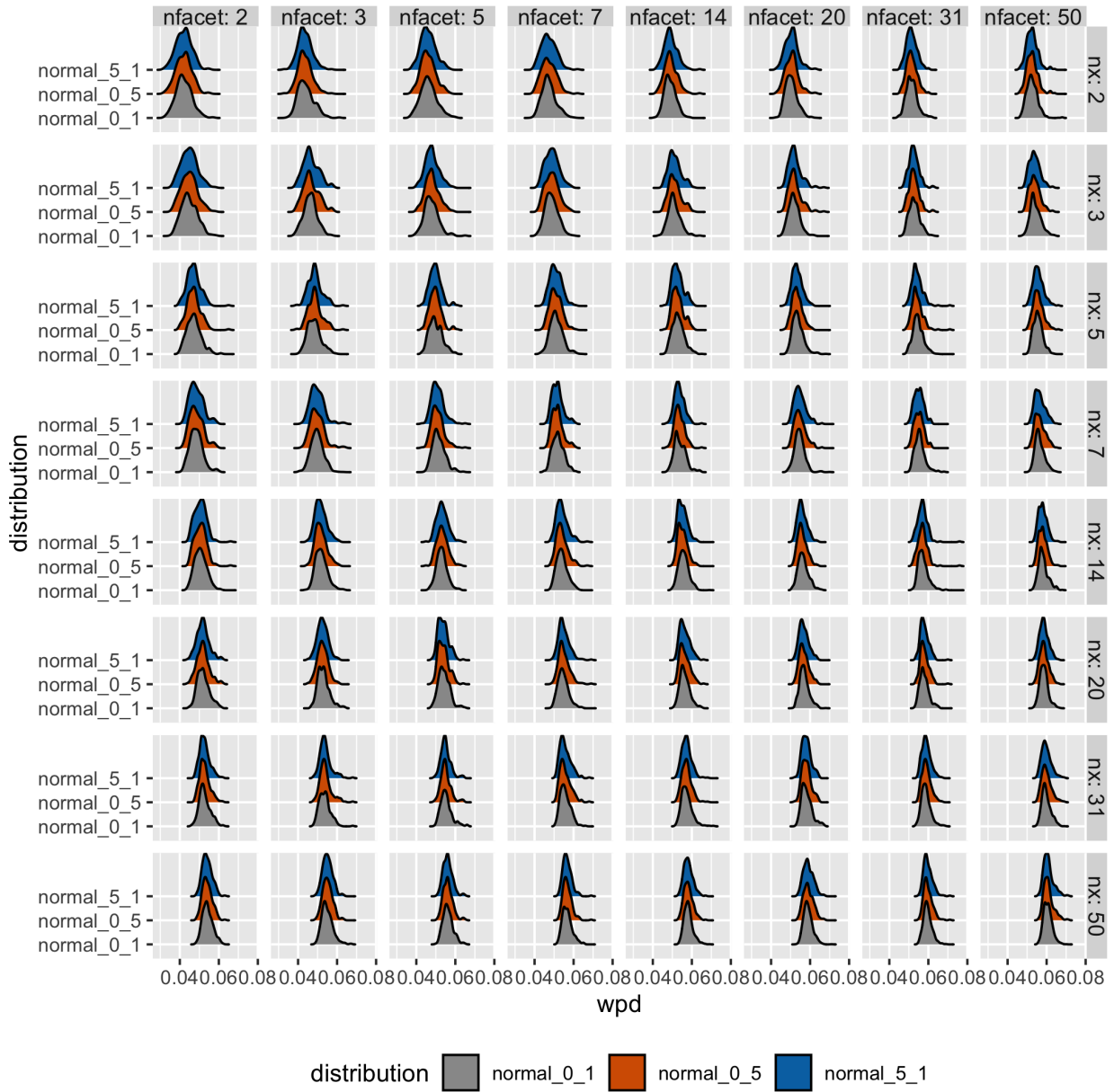


Figure 5: Ridge plots of raw wpd is shown for $N(0,1)$, $N(5,1)$ and $N(0,5)$ distribution. The densities change across different facet and x levels but look same for each panel, which implies wpd value is unaffected by the change in mean and standard deviation of the normal distribution.

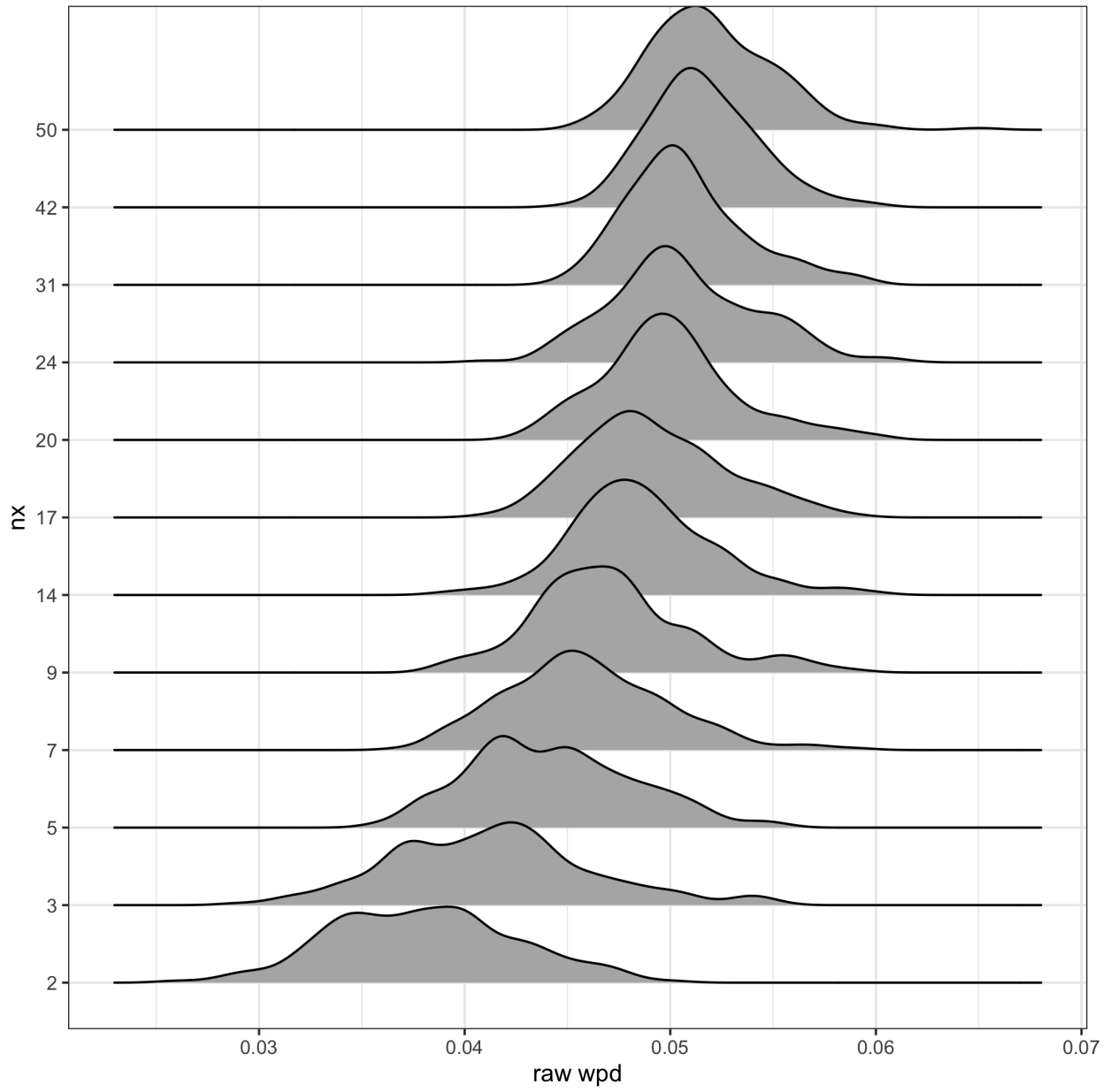


Figure 6: Ridge plots of raw wpd is shown for $N(0,1)$ distribution. For each panel, it could be seen that the location shifts to the right for increasing x levels. Across each panel, the scale of the distribution seems to change for low/moderately lower values and higher values of nfacets and left tails are longer for lower facet levels.

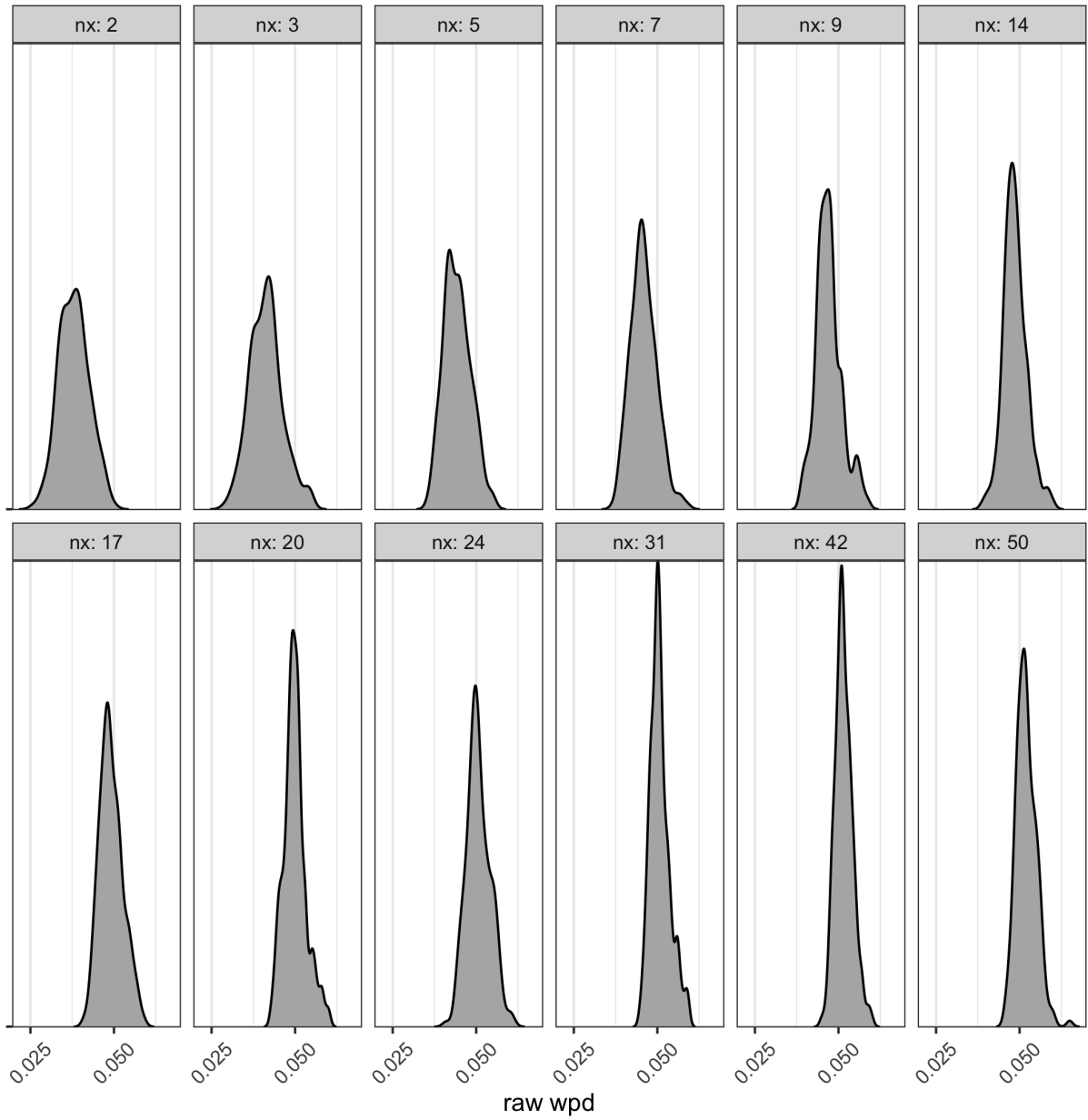


Figure 7: Ridge plots of raw wpd is shown for $N(0,1)$ distribution. For each panel, it could be seen that the peakedness shifts for increasing x levels.

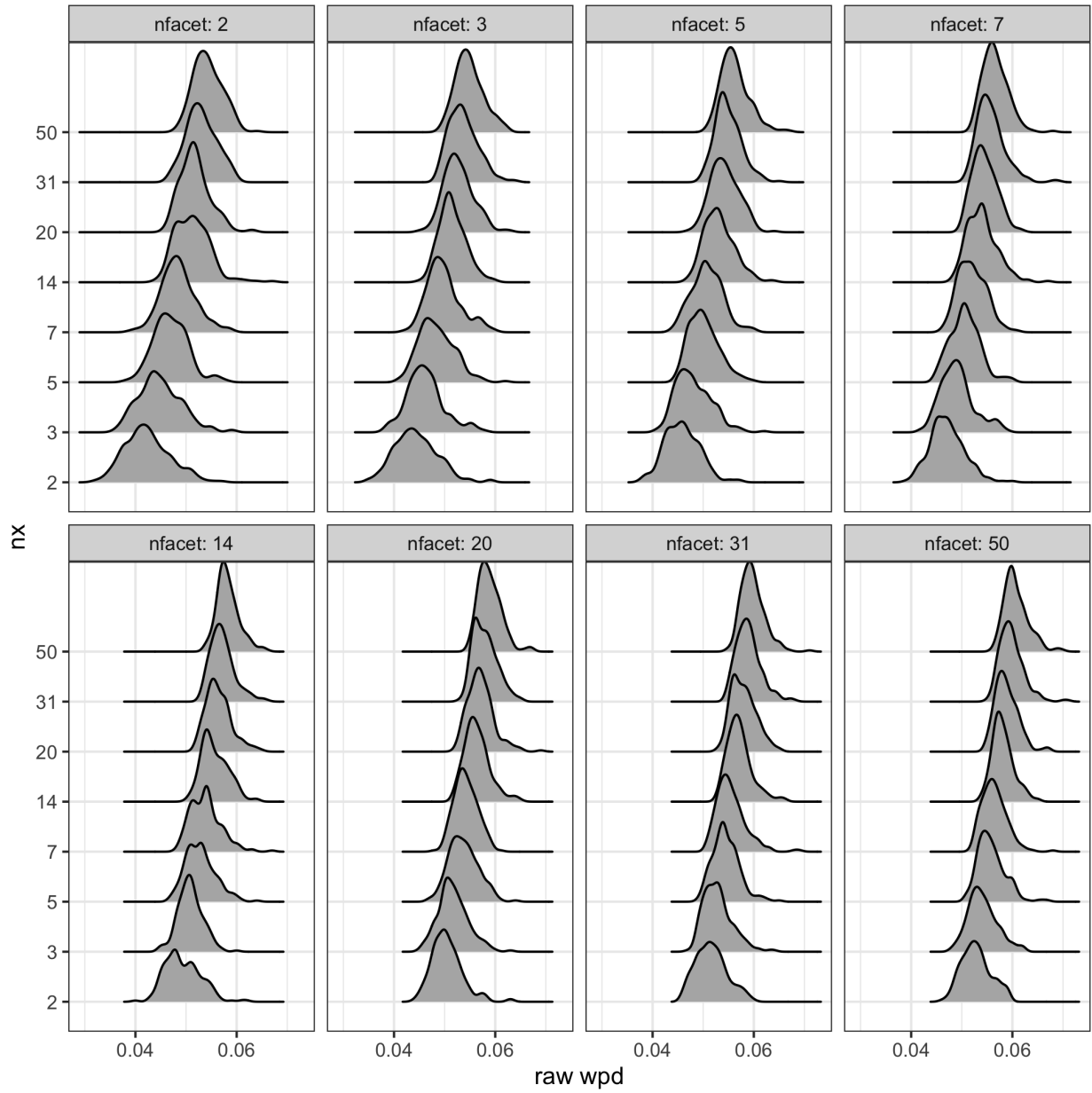


Figure 8: Ridge plots of raw wpd is shown for $N(0,1)$ distribution with $nfacets$ as facets. For each panel, it could be seen that the location shifts to the right for increasing nx levels.

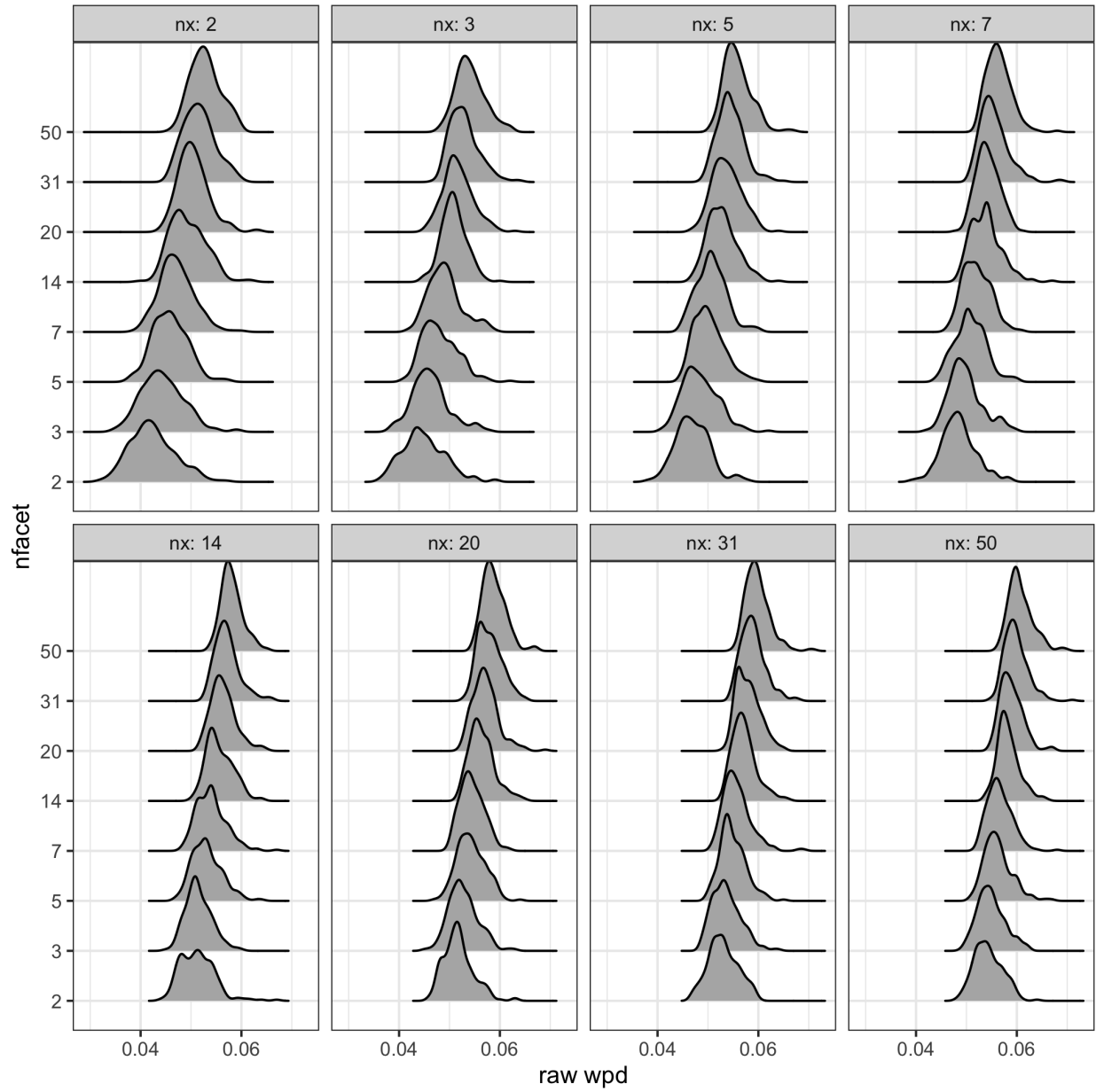


Figure 9: Ridge plots of raw wpd is shown for $N(0,1)$ distribution with nx as facets. For each panel, it could be seen that the location shifts to the right for increasing $nfacet$ levels.

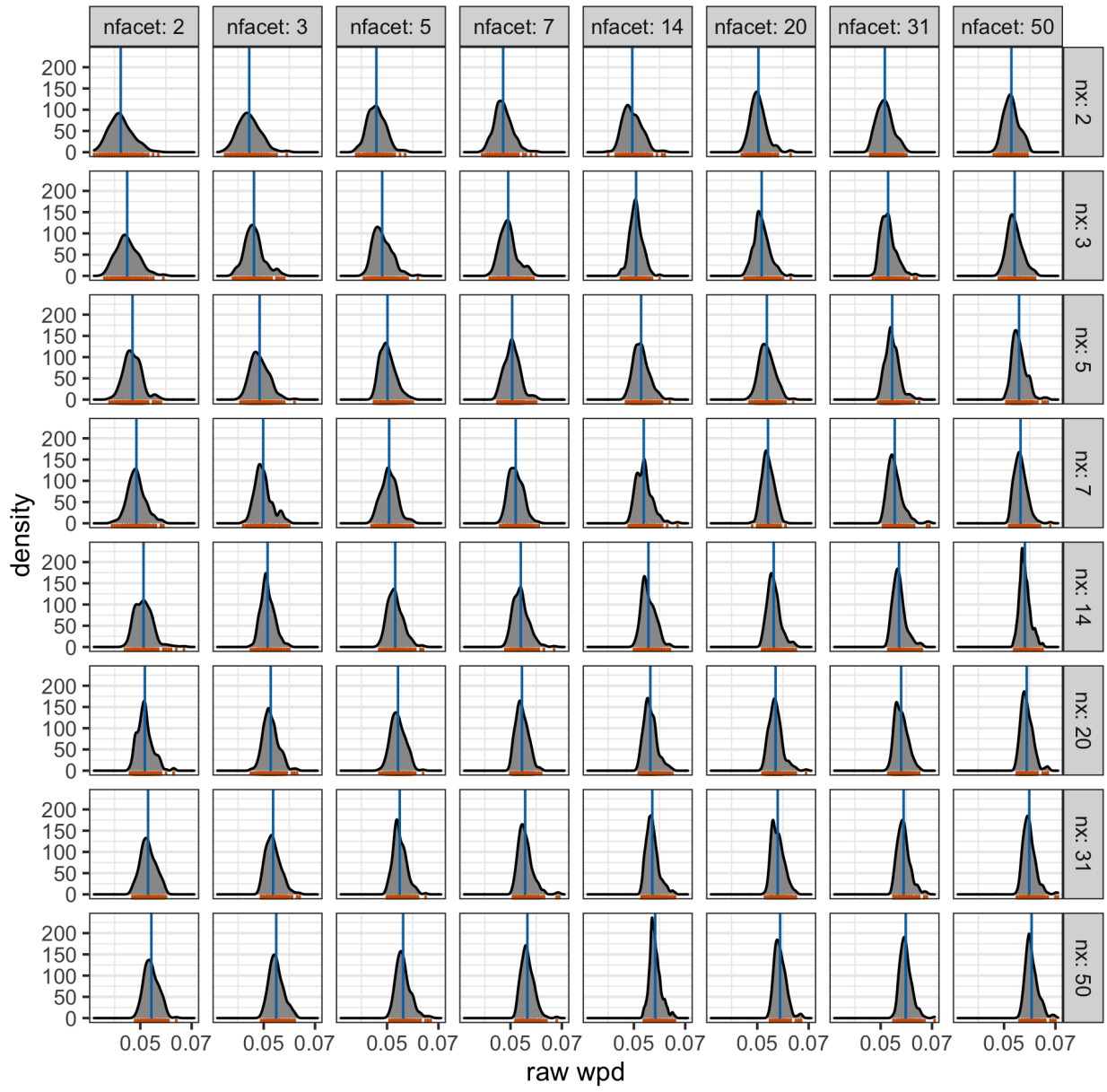


Figure 10: Density plot of raw wpd is shown for $N(0,1)$ distribution with nx on x-axis and $nfacet$ on facets. For each panel, it could be seen that the location as well as scale shifts as we move from top-left to bottom-right corner.

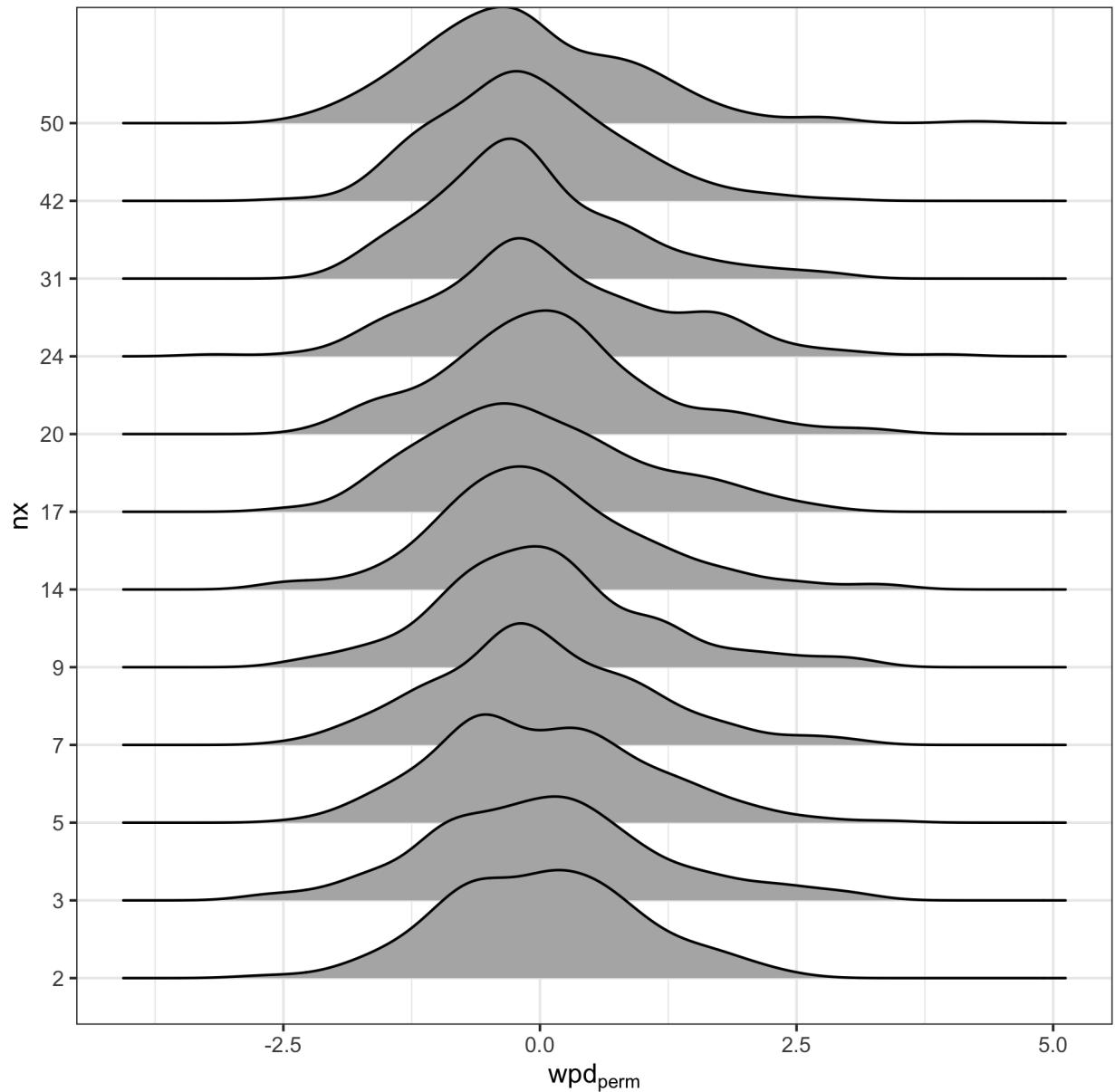


Figure 11: Distribution of wpd_{perm} are shown for different levels for $m = 1$ under the null design. The distribution for different panels have similar location and scale.

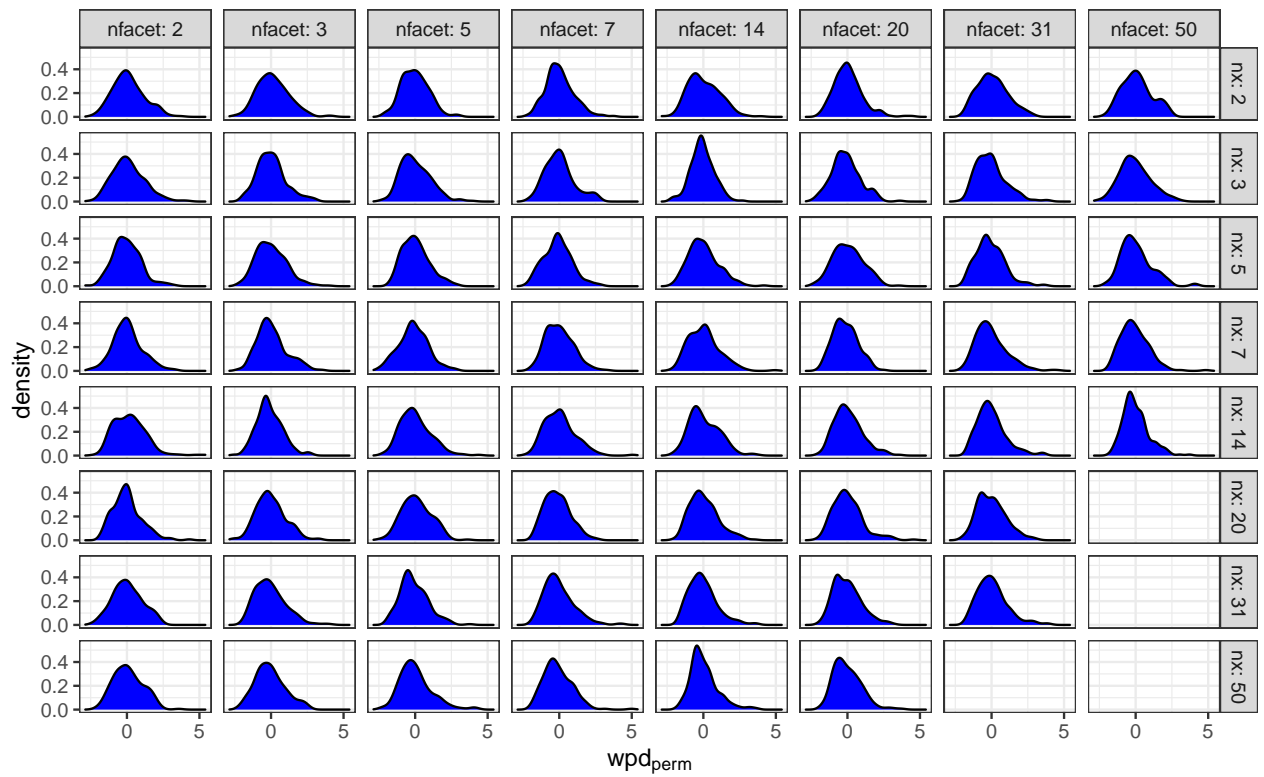


Figure 12: Distribution of wpd_{perm} are shown for different levels for $m = 2$ under the null design. The distribution for different panels have similar location and scale.

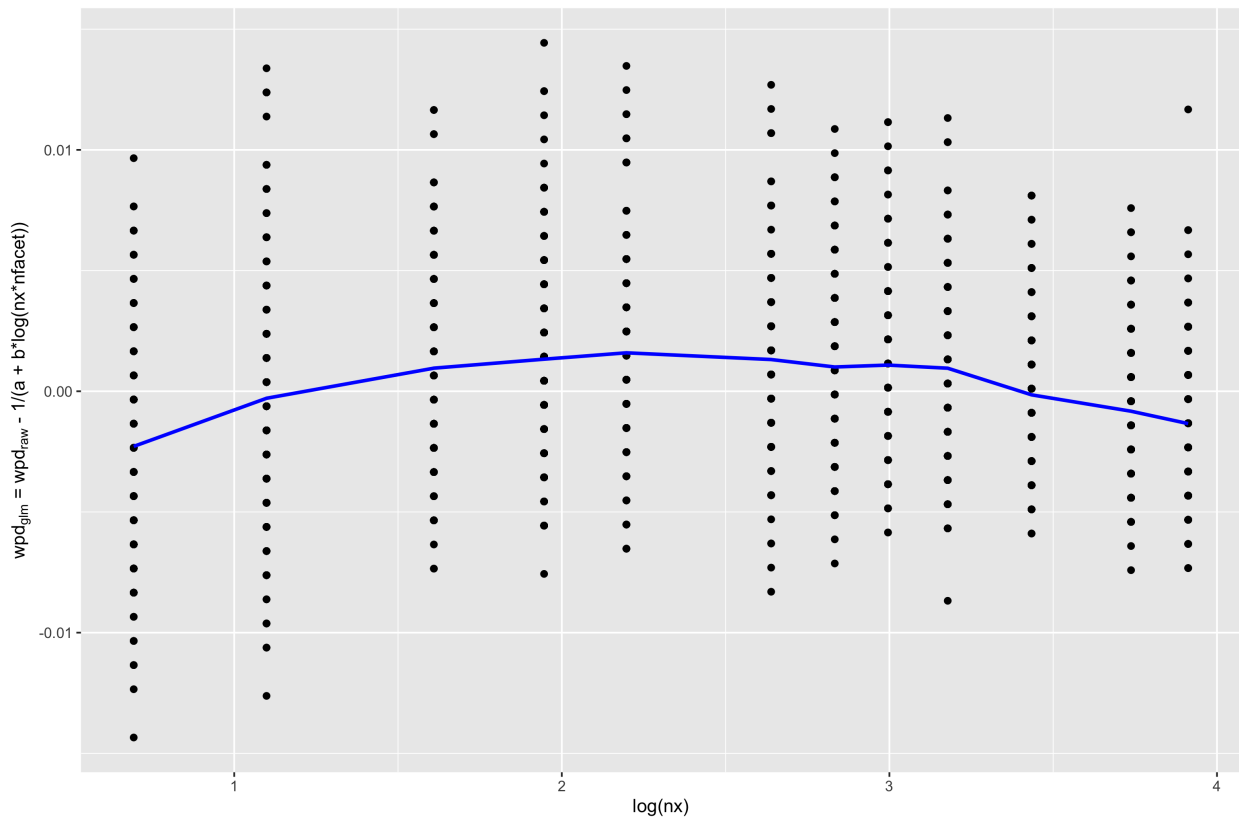


Figure 13: Residuals from the model is plotted across different number of comparisons for $m = 1$. Residuals seem to be independent of nx and have been defined as wpd_{glm} .

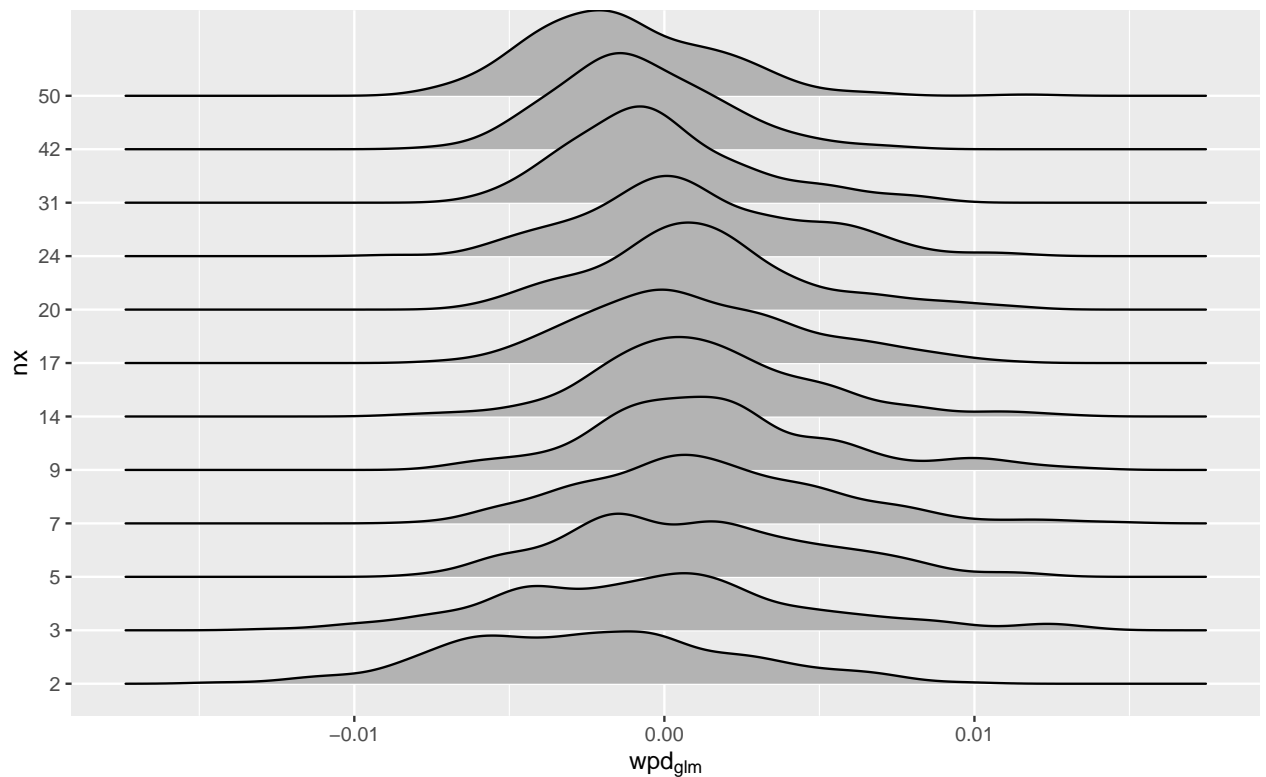


Figure 14: Distribution of wpd_{glm} is plotted across different nx for $m = 1$. Both shape and scale of the distributions are different for lower nx than for higher nx .

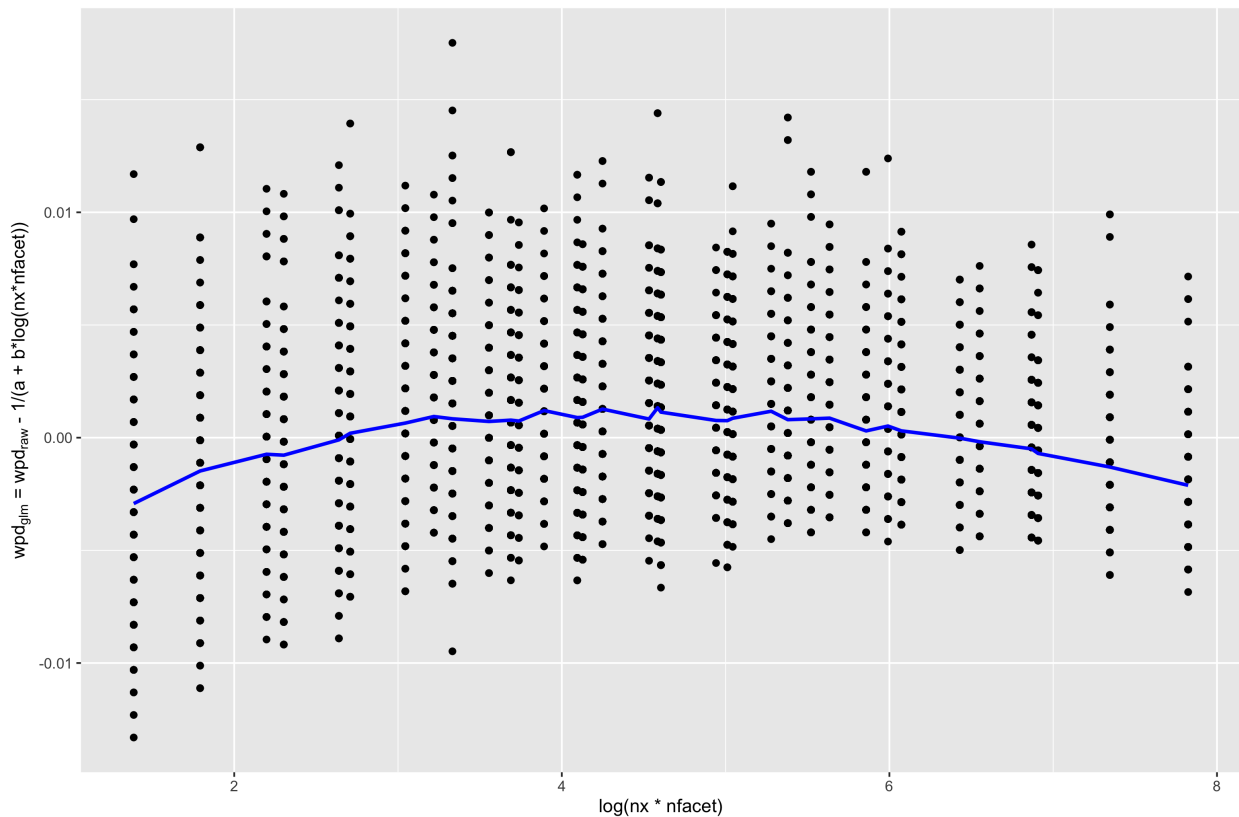


Figure 15: Residuals from the model is plotted across different number of comparisons for $m = 2$. Residuals seem to be independent of nx and have been defined as wpd_{glm} .

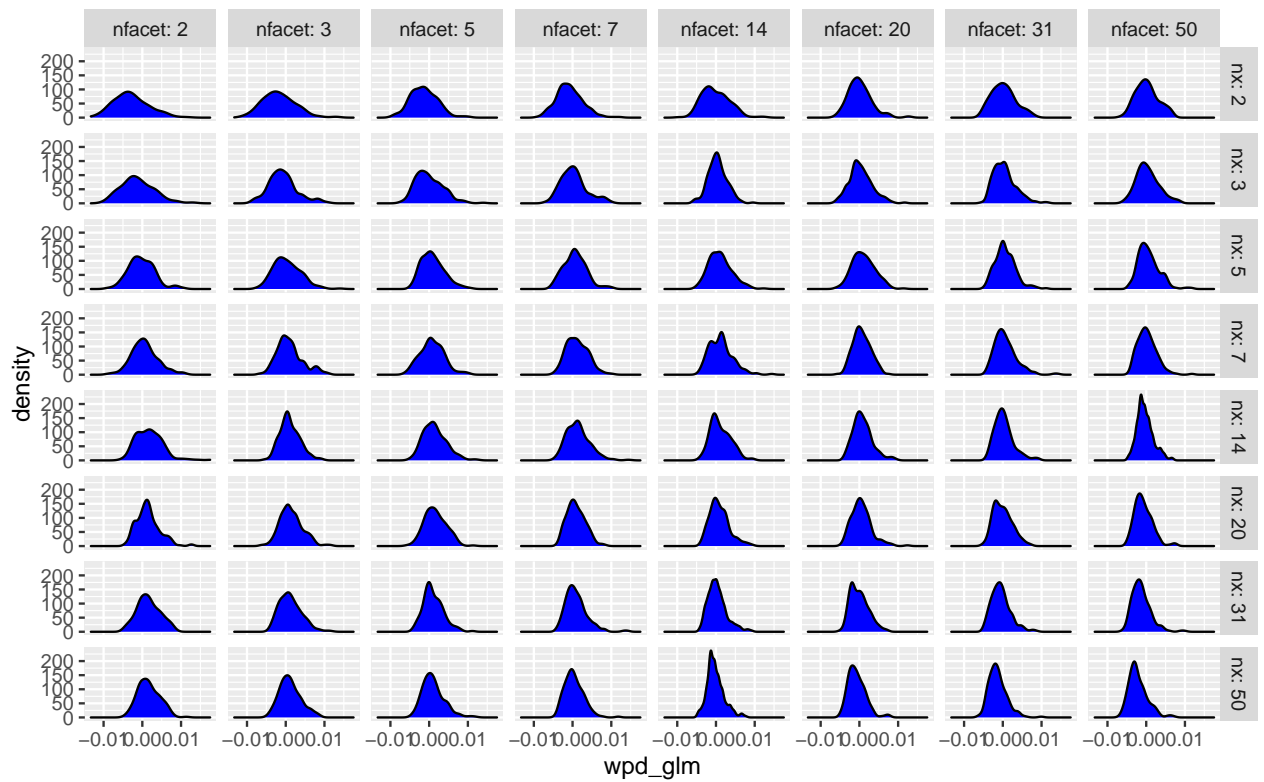


Figure 16: Distribution of wpd_{glm} is plotted across different nx for $m = 2$. Both shape and scale of the distributions are different for lower nx than for higher nx .

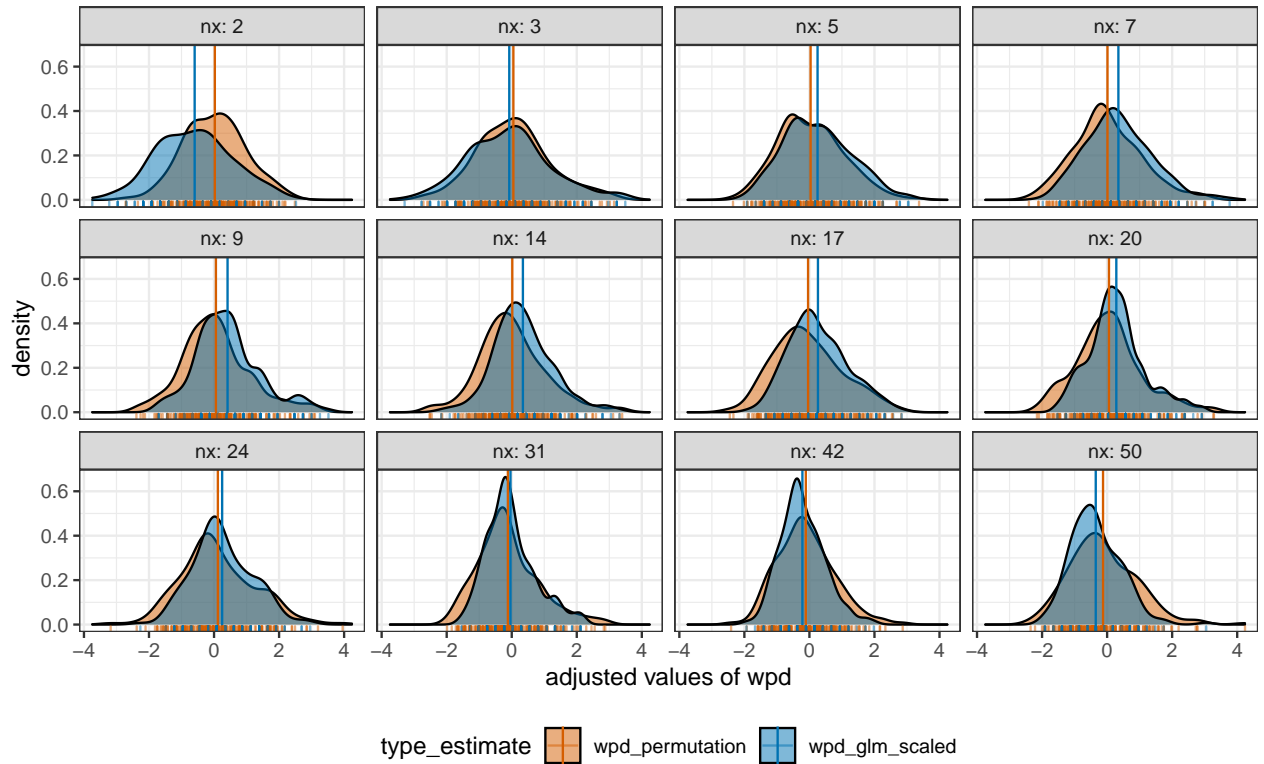


Figure 17: The distribution of wpd_{perm} and $wpd_{glm-scaled}$ are overlaid to compare the location and scale across different nx for $m = 1$. The distribution of the adjusted measure looks similar for both approaches for higher levels.

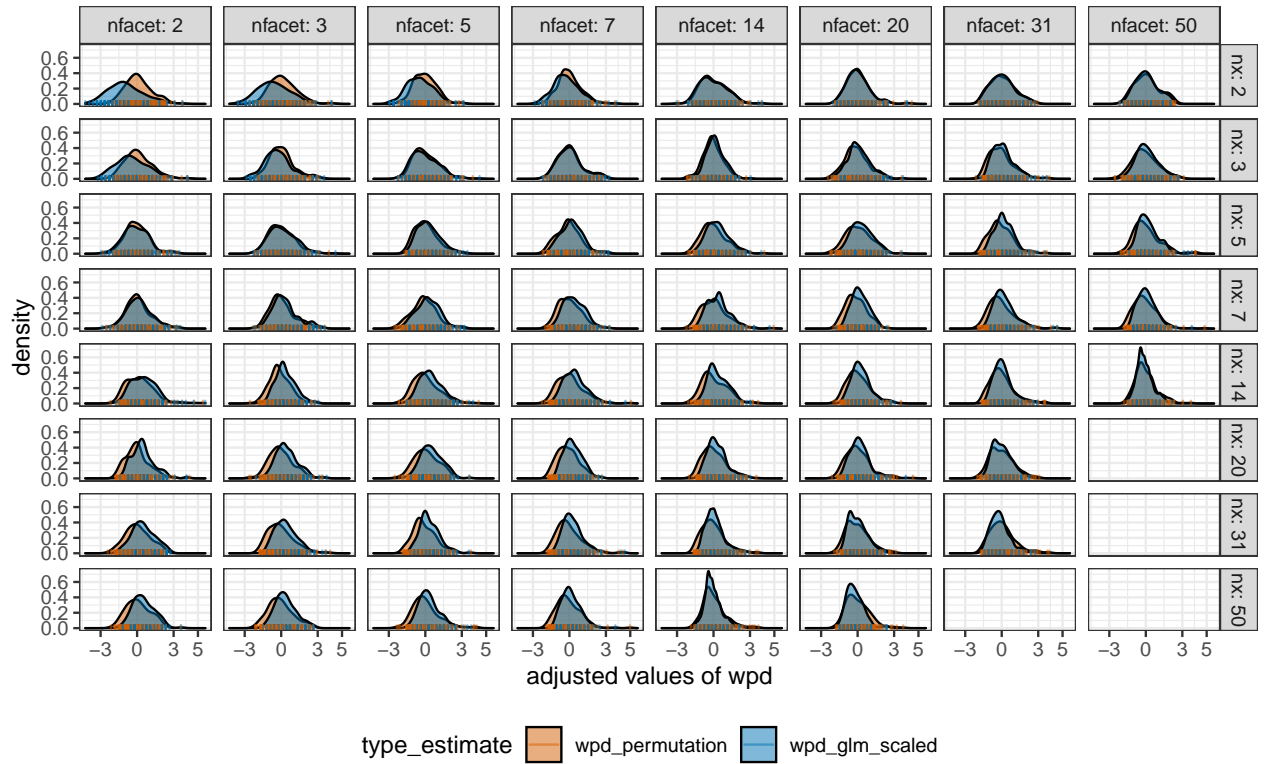


Figure 18: The distribution of wpd_{perm} and $wpd_{glm-scaled}$ are overlaid to compare the location and scale across different nx and $nfacet$ for $m = 2$. wpd_{norm} takes the value of wpd_{perm} for lower levels, and $wpd_{glm-scaled}$ for higher levels to alleviate the problem of computational time in permutation approaches. This is possible as the distribution of the adjusted measure looks similar for both approaches for higher levels.

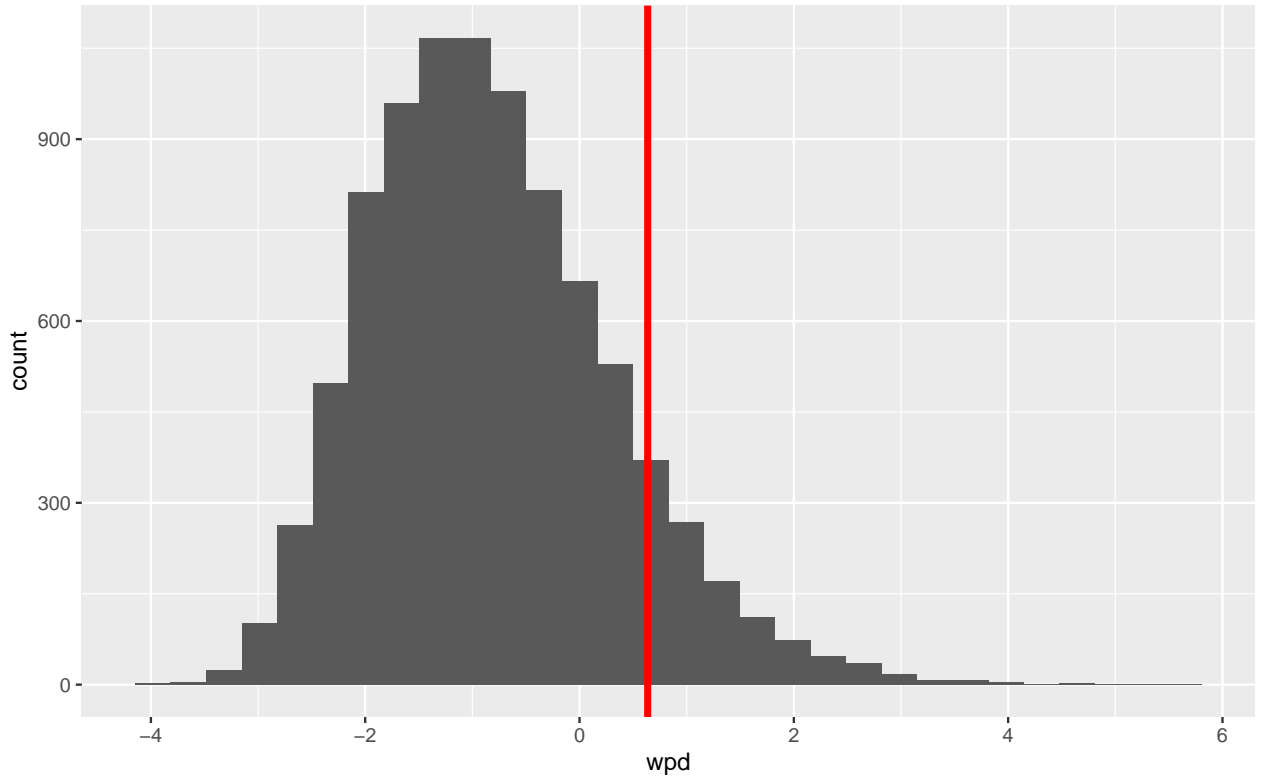


Figure 19: The distribution of wpd for 9 null designs of different levels with each harmony being rejected if the corresponding wpd value is higher than $wpd_{threshold99}$. Although the level of significance for each test is 1%, the level of significance for multiple tests together is 10% as displayed through the red line. This means 10% of the times the null designs will be tagged as interesting even when there is actually nothing interesting going on.